

# Image restoration involving connectedness

Simon Masnou and Jean-Michel Morel

Centre de Recherches en Mathématiques de la Décision (CEREMADE)  
Université Paris-IX Dauphine, 75775 Paris Cedex 16, France

## ABSTRACT

Two local adaptative nonlinear filters for image denoising are described and compared to other methods. The first one is a median filter computed over a connected neighborhood that fits the local conformation of level lines. The second one deals with the size of grains in image. Both filters depend on a single parameter, the area  $A$ , are morphological and associated with smooth as well as unsmooth fixed points. They make the total variation decrease and are able more than other classic morphological filters to denoise while preserving image structures. They are particularly designed for automation.

**Keywords:** Local adaptative morphological filtering, blind restoration, additive or impulse noise, connectedness, smooth and unsmooth fixed point, automation.

## 1. INTRODUCTION

Image restoration is essentially concerned with the following problem: what has to be kept in an image and what can be considered as noise ? But noise is generally image-sensor dependent so that no global mathematical formalization is possible. Assuming no *a priori* knowledge or estimate on the statistics of noise, we shall consequently restrain our analysis to those kinds of noise that do not involve any specific geometric pattern and are defined by a random process like Gaussian or uniformly distributed additive white noises or impulse noises. Moreover, we shall define restoration of so-corrupted images as a way of discriminating between “coherent” data (which must be preserved) and “non coherent” data (which should be modified). By “coherence” we mean that gray level at each point of an image can be in some way related to gray levels in a neighborhood of this point. We are therefore interested in local filtering.

Local filtering techniques have been widely studied in recent years, under both analytic and geometric considerations within a framework of axiomatization.<sup>1</sup> Most of the ones involving no *a priori* knowledge on noise are based on the assumption that “edges” are primitives of an image and have consequently to be detected and enhanced, whereas regions they enclose must be strongly smoothed. This approach, due to Marr and Hildreth,<sup>2</sup> resulted in most of the linear<sup>3,4</sup> and non-linear<sup>5-7</sup> filters encountered in image restoration. However “edges” are no reliable data: by definition they relate to the gray level scale, which is not representative of an image. Indeed, two different sensors capturing the same scene may produce two images with different gray level scales whereas basic information (shapes for instance) remains the same. Therefore, any filter based on edge detection may not yield the same result for the two images, assuming of course that parameters remain the same.

This remark, due to the Mathematical Morphology school,<sup>8,9</sup> led to a new class of filters – the morphological filters – which are invariant with respect to any increasing contrast change. They are closely related to the level sets (or equivalently to level lines, the boundaries of level sets) defined for every image  $u : \Omega \subset \mathbb{R}^2 \rightarrow \mathbb{R}$  by  $X_t u = \{x \in \Omega, u(x) \geq t\}$ ,  $t \in \mathbb{R}$ . The family of level sets is a morphological and complete representation of  $u$ ,<sup>10</sup> and thereby much more reliable than the set of regions enclosed by edges. Furthermore, there is an intrinsic and very natural link between level sets and shapes in image.<sup>11</sup> Since any reliable method for image restoration must be shape-oriented, we shall develop our filters within the framework of morphological denoising.

In Refs. 6,12, Leonid Yaroslavsky developed a synthetic approach to local filtering techniques based on smoothing over some neighborhood. He noticed that this neighborhood can be basically defined with two selecting criteria: a spatial criterion so that filtering be local and a brightness criterion in order to select only points which are similar in some sense – belonging to the same shape for instance. Two types of neighborhoods generically arise from this point of view:

---

Send correspondence to Simon Masnou (Email : masnou@ceremade.dauphine.fr)

1. Neighborhoods defined at each point  $x$  of image  $u$  as a subset of a disk  $B_a(x)$  with radius  $a$  under constraints on the maximal variation in the brightness domain and which can be generically defined by:

$$N_1(x) = \{y \in B_a(x), u(x) - \epsilon_v^- \leq u(y) \leq u(x) + \epsilon_v^+\}$$

2. Neighborhoods defined at  $x$  as a subset of  $B_a(x)$  under constraints on the maximal variation within variational row (the set of all points of the disk ordered with respect to their gray level values). Generic definition can be written in the discrete plane as

$$N_2(i, j) = \{(k, l) \in B_a(i, j), R(u_{i,j}) - \epsilon_R^- \leq R(u_{k,l}) \leq R(u_{i,j}) + \epsilon_R^+\}$$

where  $R(\cdot)$  denotes rank within variational row, and in the continuous plane ( $|S|$  denotes the area of set  $S$ )

$$\begin{aligned} N_2(x) = & \{y \in B_a(x), u(y) \leq u(x), |\{z \in B_a(x), u(y) \leq u(z) \leq u(x)\}| \leq \epsilon_R^-\} \cup \\ & \{y \in B_a(x), u(y) \geq u(x), |\{z \in B_a(x), u(x) \leq u(z) \leq u(y)\}| \leq \epsilon_R^+\} \end{aligned}$$

A smoothing filter (median, mean, inf, sup and all weighted derived operators) can afterwards be computed over the selected neighborhood. Of course this formalization is generic and some filters cannot be strictly described such a way, like the following operator, Susan (Smallest Univalue Segment Assimilating Nucleus) filter, introduced in Ref. 7:

$$\text{Susan } u(x) = C \int_{B_a(x)} u(y) e^{-\frac{|y-x|^2}{d^2}} e^{-\frac{|u(y)-u(x)|^2}{t^2}} dy \quad \text{where } C = 1 / \left( \int_{B_a(x)} e^{-\frac{|y-x|^2}{d^2}} e^{-\frac{|u(y)-u(x)|^2}{t^2}} dy \right)$$

and  $a$  is taken large enough so that spatial limitation be mainly due to the term  $e^{-\frac{|y-x|^2}{d^2}}$ . In view of Yaroslavsky neighborhoods, this operator can be seen as the average over a neighborhood derived from  $N_1(x)$  by weighting in both spatial and brightness domains. Susan filter shall be considered in the sequel as a reference filter – a synthesis – among those local, non-linear and non-morphological operators that involve average.

Almost every local filter, linear or non-linear, morphological or not, has generally to be iterated before it yields the desired solution. But too many iterations may result in a much too smooth image. Moreover, smoothing effect occurs even for initial smooth data. This is particularly confusing since the goal of image restoration is generally to denoise while preserving uncorrupted data. The lack of preservation is actually due to the definition of coherence which is implicitly related to each filter. Let us say that an image is coherent with respect to some operator if it is a fixed point for this operator.

For instance, every filter based on the Hildreth–Marr approach implicitly defines a coherent image as made of pieces in which local variation of brightness is small and regular and such that this variation is larger than some threshold between two connected pieces. A coherent image with respect to the conventional median filter (the morphological reference filter) in the continuous plane is such that curvature is zero at every point of any level line.<sup>10</sup> If it is with respect to the median filter computed over some  $N_2$ -like neighborhood, then the curvature at any point of any level line must not exceed some upper limit.<sup>13</sup> On the discrete grid these last two conditions can be weakened due to numerical approximations. But the classes of coherent images with respect to both operators are still restricted to smooth images (the larger the size of working window, the smoother the image). Therefore, iterating one of these filters on a “natural” image until convergence often yields a result that is too smooth to be satisfactory.

Figure 1 illustrates why conventional median filter and median filter computed over some  $N_2$ -like neighborhood are associated with such a restricted class of coherent images: they involve a neighborhood that cannot fully fit the local conformation of level lines for it is constrained inside a disk.<sup>13</sup> Now, is there a way to remove spatial constraint while letting filtering be local ? Simplest answer seems to be connectedness.

## 2. MEDIAN FILTER ON CONNECTED NEIGHBORHOOD (MFCN)

Since  $N_1$ -like neighborhoods are not morphological, we shall concentrate our study on local filtering involving  $N_2$ -like neighborhoods. We now examine how the definition of the Yaroslavsky set  $N_2$  can be modified so that connectedness be involved. Recall that  $N_2(x)$  is made of two subsets of a disk. A “monotone” set of area  $\epsilon_R^+$  made of points with gray level larger than  $u(x)$  and a “monotone” set of area  $\epsilon_R^-$  made of points with gray level less than  $u(x)$ . By “monotone”

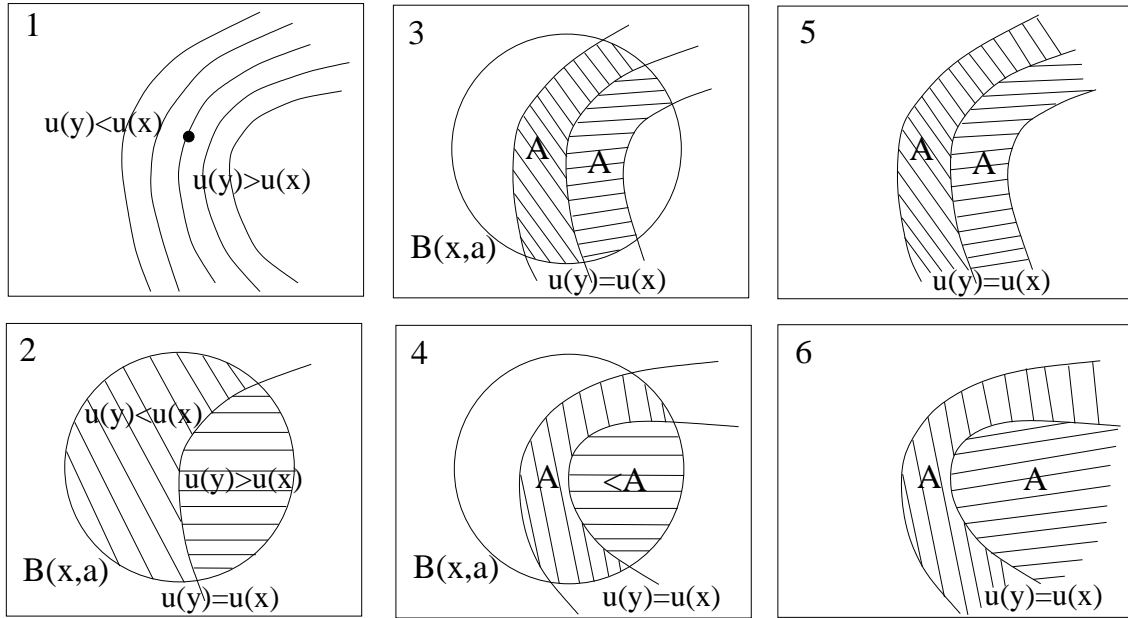


**Figure 1.** The evolution of a regular function at a regular point (1) can be avoided only by removing spatial constraint

2] Conventional median filter: evolution of level line  $u(y) = u(x)$  as soon as  $|\text{curv } u(x)| > 0$ .

(indeed  $|\{y, u(y) > u(x)\}| < |\{y, u(y) < u(x)\}|$ )

3-4] Median filter applied on  $N_2$ -like neighborhood: evolution as soon as  $|\text{curv } u(x)| > C$ .

5-6] Median filter on connected neighborhood: no evolution  $\forall \text{curv } u(x)$ .

we mean that  $N_2(x)$  can be constructed by progressively adding points  $y$  with respect to the distance  $|u(y) - u(x)|$  (the lower this distance, the sooner  $y$  is added). The way we shall construct our neighborhood is equivalent, except that we combine the “monotone” characteristic of set with connectedness and that we posit  $A := \epsilon_R^+ = \epsilon_R^-$ . The most natural way of doing this is the following.

Let  $\mathcal{W}_\mu^-$  be the set of all points  $y$  such that  $\mu \leq u(y) \leq u(x)$  and for every  $\mu \leq u(x)$  we define  $W_\mu^-$  as the connected component of  $x$  in  $\mathcal{W}_\mu^-$  (i.e. the maximal connected subset of  $\mathcal{W}_\mu^-$  containing  $x$ ).

Then, assuming for the sake of simplicity that  $W_{u(x)}^-$  is of area less than  $A$  (general point of view shall be respected later), we define  $\lambda := \inf\{\mu \leq u(x), |W_\mu^-| \leq A\}$ . If  $\lambda > -\infty$  and  $|W_\lambda^-| < A$ , the situation is as illustrated in Figure 2. The set  $W^-$  whose area equals  $A$  and such that  $W_\lambda^- \subset W^- \subset W_{\lambda-1}^-$  is constructed by selecting points in  $W_{\lambda-1}^- \setminus W_\lambda^-$  with respect to the geodesic distance to  $W_\lambda^-$  within  $W_{\lambda-1}^-$ . This way of proceeding is much more natural than taking the distance to  $x$  since it involves the shape of  $W_\lambda^-$ .

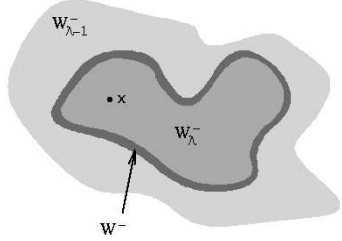


**Figure 2.** If  $|W_\lambda^-| < A$  and  $|W_{\lambda-1}^-| > A$ , the set  $W^-$  such that  $|W^-| = A$  is constructed with respect to the geodesic distance to  $W_\lambda^-$  within  $W_{\lambda-1}^-$ .

If now  $\lambda = -\infty$  or  $|W_\lambda^-| = A$  we simply define  $W^- = W_\lambda^-$ .

The set  $W^+$  can be constructed exactly the same way by taking into account points having a gray level larger than  $u(x)$ . The main advantage of both sets  $W^-$  and  $W^+$  is their property to fit perfectly the local conformation of level lines as illustrated in Figure 3 (the set  $W^=$  denotes the connected component of  $x$  within the set  $\{y, u(y) = u(x)\}$  – naturally  $W^= \subset W^+$  and  $W^= \subset W^-$ ).

We shall say that an image  $u$  defined on  $\Omega \subset \mathbb{R}^2$  is locally  $A$ -coherent if for every point of  $\Omega$ ,  $|W^-| = |W^+| = A$ . Of course any  $u$  defined on  $\Omega$  is at least 0-coherent. With such a definition,  $A$  is in some way the scale at which we

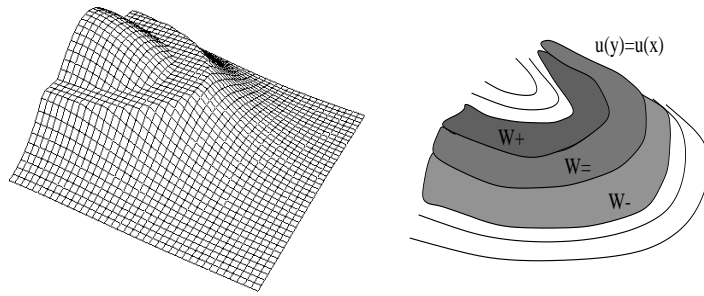


**Figure 3.**  $W^-(x)$ ,  $W^=(x)$  and  $W^+(x)$  on a formal example  
 Left : 3D plot of a smooth function – Right : shapes of  $W^-(x)$ ,  $W^=(x)$  and  $W^+(x)$

check out coherence. But here coherence takes into account only the ordering of gray level values (in contrast to non-morphological definitions) and does not involve any restriction on the shape of level sets (in contrast to conventional median filter or median filter computed over  $N_2$ -like neighborhoods). Now which morphological operator shall be used so that any  $A$ -coherent image be a fixed point ? The simplest filter satisfying this property is median filter, so that we define our Median Filter on Connected Neighborhood ( $\text{MFCN}$ ) with scale  $A$  by

$$\text{MFCN}_A u(x) = \inf\{\lambda, |\{y \in W^- \cup W^+, u(y) \leq \lambda\}| \geq \frac{|W^- \cup W^+|}{2}\}$$

It is easily seen that if  $|W^-| = |W^+| = A$  then  $\text{MFCN}_A u = u(x)$  so that any  $A$ -coherent image  $u$  is a fixed point for  $\text{MFCN}_A$ . This class of coherent images is much bigger than the classes of fixed points related to classic local filters; therefore  $\text{MFCN}_A$  shall be able to preserve regular data much better than these filters.

Actually, the rough definition we gave for  $W^-$  and  $W^+$  is not satisfactory. The two functions  $u_1$  and  $u_2$  illustrated in Figure 4 are equal up to some saturation effect (which characterizes any image sensor). Since  $A$  is larger than the area of set  $M$  made of points modified by truncation,  $\text{MFCN}_A$  should yield the same result for  $u_1$  and  $u_2$ , which is not the case. This is due to the relation  $|W^-| = |W^+| = \frac{A+1}{2} > |W^- \setminus W^=|$  satisfied at any point  $x$  of  $M$  so that  $\text{MFCN}_A u_2(x) = u_2(x)$ .

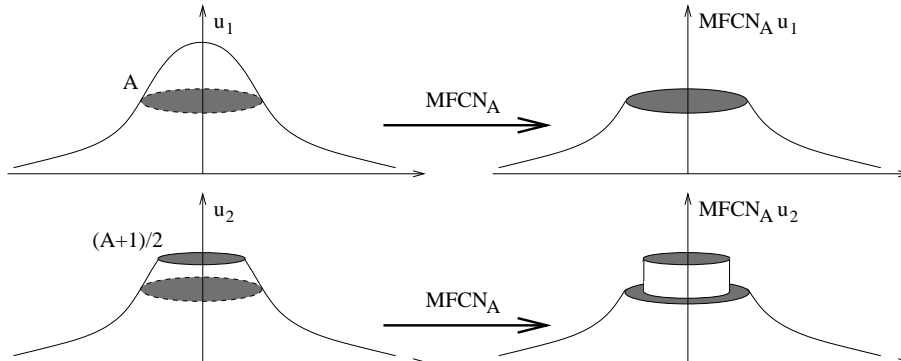


**Figure 4.**  
 Saturation effect is not properly processed by  $\text{MFCN}$  ( $\text{MFCN}_A u_1$  and  $\text{MFCN}_A u_2$  denote actually the results obtained after several iterations until convergence).

The algorithm that we are now going to describe is a way to get rid of this drawback; it allows, if necessary,  $W^-$  or  $W^+$  to have an area larger than  $A$  in order to force evolution (step 5 of algorithm). More generally, the filter we define uses three types of information:

1. Area (as a way of measuring coherence).
2. Geodesic distance (to achieve if possible the exact area).
3. Area disparity between sub- and super-neighborhoods (to deal correctly with truncation effects).

**Algorithm** (this version is not optimal but understandable):

```

level_min ← inf  $u_{i,j}$  ; level_max ← sup  $u_{i,j}$ .
For ( $n \leftarrow 1$ ;  $n \leq$  number of iterations;  $n \leftarrow n + 1$ )
  ( $i, j$ ) ← first point of image
  1 Compute  $W^=$ 
   $W^=$  ← connected component of  $(i, j)$  in  $\{(k, l), u_{k,l} = u_{i,j}\}$ 
  If  $|W^=| \geq A$  then  $out_{i,j} \leftarrow u_{i,j}$  ; Goto 7 ( $|W^=| \geq A \Rightarrow W^- \subset W^=$  and  $W^+ \subset W^=$  so that  $\text{med}_{W^- \cup W^+} = u_{i,j}$ )
  2 Compute  $W^-$ 
  level ←  $u_{i,j}$  ;  $W_{\text{level}}^- \leftarrow W^=$ 
  While  $|W_{\text{level}}^-| < A$  and level  $\geq$  level_min do
     $W_{\text{level}}^-$  = connected component of  $(i, j)$  in  $\{(k, l), \text{level} \leq u_{k,l} \leq u_{i,j}\}$ 
    level ← level - 1
  If level < level_min then level ← level_min
   $W^- \leftarrow W_{\text{level}}^-$ 

  3 Compute  $W^+$ 
  level ←  $u_{i,j}$  ;  $W_{\text{level}}^+ \leftarrow W^=$ 
  While  $|W_{\text{level}}^+| < A$  and level  $\leq$  level_max do
     $W_{\text{level}}^+$  ← connected component of  $(i, j)$  in  $\{(k, l), u_{i,j} \leq u_{k,l} \leq \text{level}\}$ 
    level ← level + 1
  If level > level_max then level ← level_max
   $W^+ \leftarrow W_{\text{level}}^+$ 

  4 If  $|W^-| \geq A$  and  $|W^+| \geq A$  then  $out_{i,j} \leftarrow u_{i,j}$  ; Goto 7

  5 If  $|W^-| \geq A$  and  $|W^+| < A$ 
    level ←  $u_{i,j}$  ;  $W_{\text{level}}^- \leftarrow W^=$ 
    While  $|W_{\text{level}}^- \setminus W^=| < A$  and level  $\geq$  level_min do
       $W_{\text{level}}^-$  ← connected component of  $(i, j)$  in  $\{(k, l), \text{level} \leq u_{k,l} \leq u_{i,j}\}$ 
      level ← level - 1
    If level < level_min then level ← level_min
    While  $|W_{\text{level}}^- \setminus W^=| > A$  do
      Compute geodesic distance between  $W_{\text{level}+1}^-$  and every point of  $W_{\text{level}}^- \setminus W_{\text{level}+1}^-$ .
      Furthest points are removed from  $W_{\text{level}}^-$  with respect to the difference between their gray level and  $u_{i,j}$ 
      (the more different they are the sooner they are removed).
       $W^- \leftarrow W_{\text{level}}^-$ 
    Else if  $|W^-| < A$  and  $|W^+| \geq A$ 
      level ←  $u_{i,j}$  ;  $W_{\text{level}}^+ \leftarrow W^=$ 
      While  $|W_{\text{level}}^+ \setminus W^=| < A$  and level  $\leq$  level_max do
         $W_{\text{level}}^+$  ← connected component of  $(i, j)$  in  $\{(k, l), u_{i,j} \leq u_{k,l} \leq \text{level}\}$ 
        level ← level + 1
      If level > level_max then level ← level_max
      While  $|W_{\text{level}}^+ \setminus W^=| > A$  do
        Compute geodesic distance between  $W_{\text{level}-1}^+$  and every point of  $W_{\text{level}}^+ \setminus W_{\text{level}-1}^+$ .
        Furthest points are removed from  $W_{\text{level}}^+$  with respect to the difference between their gray level and  $u_{i,j}$ 
        (the more different they are the sooner they are removed).
         $W^+ \leftarrow W_{\text{level}}^+$ 
    6 Define  $W \leftarrow W^- \cup W^+$ ;  $out_{i,j} \leftarrow \text{median}(W)$ 

    7 If possible  $(i, j) \leftarrow$  next point
    Else for each point  $(i, j)$  of image,  $u_{i,j} \leftarrow out_{i,j}$  ; Next iteration.
  
```

Properties of  $\text{MFCN}$  defined by previous algorithm are the following (see Ref. 13 for a definition of  $\text{MFCN}$  as an operator acting on the space  $\text{BV}$  of functions of bounded variations mapping  $\mathbb{R}^2$  onto  $\mathbb{R}$  and for proofs):

1.  $\text{MFCN}$  is morphological. Indeed, points are taken into account with respect to their only gray level ordering ( $u(z) < u(y) < u(x)$ ).
2.  $\text{MFCN}$  is invariant with respect to any Euclidean mapping of the plane (rotation, translation, reflection, ...).
3.  $\text{MFCN}$  makes the total variation  $\int_{\Omega} |Du|$  decrease.
4. Like almost every filter defined on the discrete grid, the sequence  $(\text{MFCN}^n u)_{n \in \mathbb{N}}$  converges after some iterations to a fixed point. But in contrast to other classic morphological filters, this solution may be unsmooth since the class of fixed points does not reduce to smooth functions. This result is particularly relevant for automation since it allows to iterate until convergence. There is finally only one parameter needed: the area  $A$ .

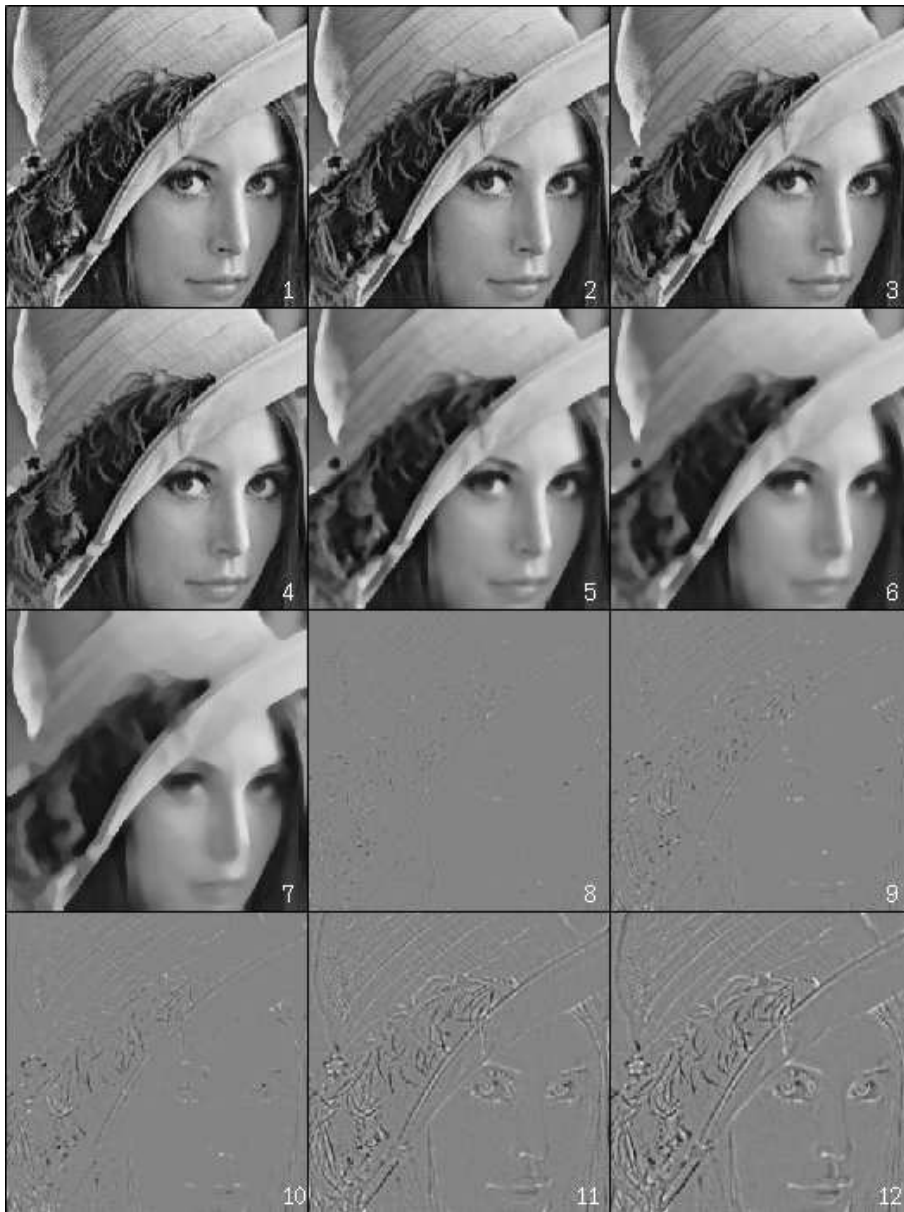


**Figure 5.**

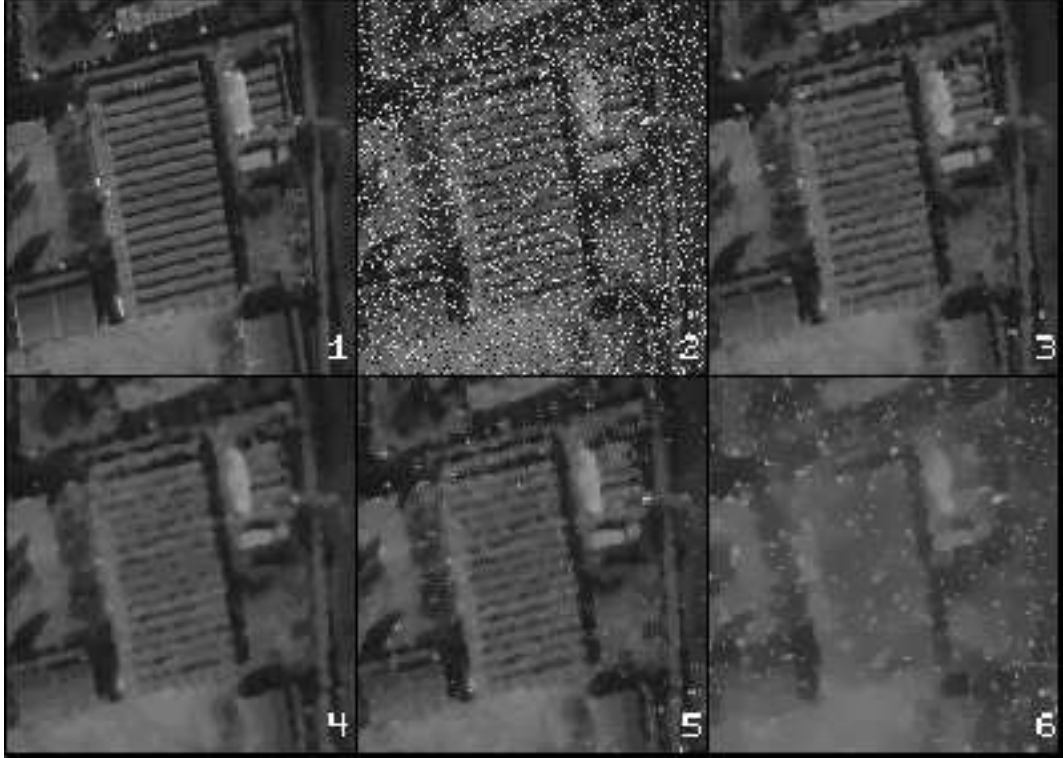
1	Original image $u$
2	$(\text{MFCN}_{10})^{11}(u)$ (fixed point)
3	$(\text{MFCN}_{20})^{10}(u)$ (fixed point)
4	$(\text{MFCN}_{30})^{10}(u)$ (fixed point)
5	$(\text{med}_{B(.,3)})^2 u$ (to be compared with [2])
6	$(\text{med}_{B(.,4)})^2 u$ (to be compared with [3])
7	$(\text{med}_{B(.,5)})^2 u$ (still no fixed point)
8-12	Normalized differences between images 2-6 and original image 1

Figure 5 is related to Property 4; it illustrates the existence of unsmooth fixed points and the remarkable stability of unnoisy data through filtering. In contrast, conventional median filter with a working window of area  $2A$  yields much too smooth solutions which are not fixed points (other classic morphological filters have exactly the same drawback). Finally we deduce from these experiments that choosing a value for parameter  $A$  (generally taken between 5 and 20) is not a drawback in contrast to most of denoising filters for which the choice is often crucial and highly delicate.

In the following experiments we compare  $\text{MFCN}$  with reference filters. Conventional median filter is taken as the reference morphological filter, Susan filter can be considered as a synthesis of classic local and non-linear filters

involving average – and therefore non morphological. We also compare **MFCN** with a global and non-linear denoising method, introduced by Rudin and Osher,<sup>14</sup> which involves a minimization of total variation  $\int |Du|$  under constraints based on an *a priori* knowledge about the statistics of noise.

Figure 6 illustrates the performances of these filters when original image (detail of an aerial CNES photograph) is corrupted by a large amount of impulse noise ( $f = 25\%$ ). The best result – which is also a fixed point in contrast to the other methods – is obviously performed by **MFCN**. This is not surprising in view of our approach. Indeed, a point is not modified through filtering if it belongs to some sub- and super-neighborhoods of same area; most of the points that do not satisfy this property are noisy points, so that filtering performs a real denoising while unnoisy points are not altered. The decay of total variation is particularly large since an impulse noise creates large and frequent variations.



**Figure 6.** 1 Original image  $u_0$  (aerial CNES photograph) 2 Noisy image  $u$  (impulse noise,  $f = 25\%$ )  
3  $(\text{MFCN}_5)^5(\text{med}_{B(.,1)}u)$  (fixed point, 4-connectivity) 4  $(\text{med}_{B(.,1.5)})^2(u)$   
5  $(\text{Susan}_{(t=12, d=0.4)})u$  6 Rudin-Osher ( $\epsilon = 1$ ,  $dt = 1$ ,  $T_0 = 0$ ,  $T = 40$ )

In contrast, the Rudin–Osher method performs quite badly for it was not designed for this kind of noise (but we are interested in blind restoration). Conventional median filter yields a solution that is too smooth when Susan filter does not succeed in removing noise (a less noisy result could be obtained but associated with a high loss of definition in image).

The ability of **MFCN** to preserve structure much better than other filters is due to its weak smoothing property. This may be a drawback on a qualitative point of view: the original lack of smoothness of level lines or the one generated by noise will remain unless a smoothing process is introduced. Take for instance the example illustrated in Figure 7. The white square is processed by **MFCN** as a noisy region because of its small area and is correctly removed. But the local “deviation” of “the” main level line due to the square has been preserved. A solution consists in computing median filter inside the only region previously occupied by the square; the smoothness of the line is then recovered without any global evolution. Drawback of this post-smoothing method is that the fixed point property is lost and that two more parameters have to be introduced: the radius of the disk on which median is computed and the number of iterations. Now let us emphasize the difference between this method and a denoising

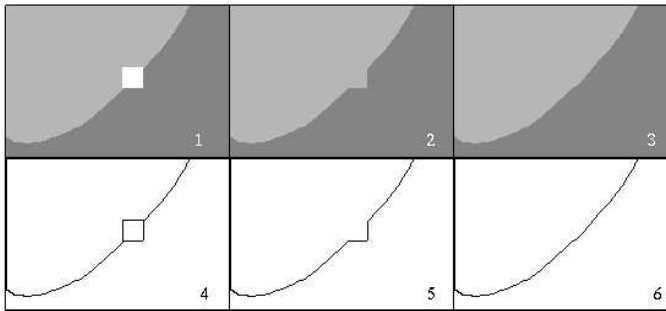


**Figure 7.**

- 1 Noisy image  $u$
- 2  $\text{MFCN}_A^n u$
- 3  $\text{Cmed}_{D(.,r)}(\text{MFCN}_A^n u)$
- 4-5-6 Level lines in images 1-2-3

with conventional iterated median filter. The latter induces a global diffusion from the only curvature of level lines. The former recovers local coherence from the area of bilevel sets – i.e.  $X_{\lambda, \nu} = \{x \in \Omega, \lambda \leq u(x) \leq \nu\}$  – and points which have been modified are considered as noisy points; they are the only points where the diffusion process occurs, so that there is no global alteration of image structures.

We currently study a morphological and idempotent (yielding a fixed point in one iteration) method that would replace the conventional iterated median for post-smoothing of modified zones. These zones may indeed be considered as occlusions and the problem of their smoothing may reduce to the minimization of some functional with Dirichlet constraints or, in other words, with constraints on the boundaries of occlusions.

Another way of obtaining a smoother result without losing the fixed point property consists in applying the conventional iterated median to the whole image before  $\text{MFCN}$ . Naturally, this pre-smoothing has to be slight in order to avoid a serious alteration of structures in image: radius of the structuring element and the number of iterations have to be small. It arises from our experiments that pre-smoothing is particularly interesting in case of images corrupted with white additive noises. The following equation synthetizes the joining of  $\text{MFCN}$  to both pre-smoothing and post-smoothing – values of disk radius and iterations number are empirically the ones offering the best compromise between smoothing and structure preservation:

$$v(.) = \text{Cmed}_{D(.,1.5)} \text{MFCN}_A^n \text{med}_{D(.,1)}(u)(.) \quad \text{where} \quad \text{Cmed}_{D(.,1.5)} \Psi u(.) = \begin{cases} \text{med}_{D(.,1.5)} \Psi u(.) & \text{if } \Psi u(.) \neq u(.) \\ \Psi u(.) & \text{else} \end{cases}$$

and  $n$  is the number of iterations until convergence. Let us however notice that we generally avoid using post-smoothing: we used for example the only pre-smoothing in Figure 6 (one iteration of median filter on a ball  $D(.,1)$ ).



**Figure 8.**

- 1 Original image
- 2 Image  $u$  corrupted with white additive Gaussian noise ( $\sigma = 10$ )
- 3  $(\text{MFCN}_{10})^6(\text{med}_{B(.,1)} u)$   
(fixed point for  $\text{MFCN}_{10}$ )
- 4  $(\text{med}_{B(.,1.5)})^2 u$
- 5 Rudin-Osher method  
( $\epsilon = 1, dt = 1, T_0 = 0, T = 6$ )
- 6 Susan<sub>(d=1.4, t=12)</sub>( $u$ )

This figure illustrates the results obtained by applying the filters described above to an image corrupted with a white Gaussian additive noise of standard deviation 10.

Rudin–Osher method performs obviously well – it was specifically designed for this type of noise – but it is not morphological, parameters are hardly adjustable, the solution is not a fixed point and too many iterations yield a piecewise constant solution made of large and artificial pieces. In contrast  $\text{MFCN}$  converges to a solution which is less fair but is a fixed point and therefore depends of only one parameter ( $A$ ). Moreover,  $\text{MFCN}$  is morphological and

yields better result than the reference conventional median filter in view of preserving structures: details are sharper and there was no global diffusion. Finally Susan filter performs well in removing noise, but the use of average filter induces a strong regularization that makes the fine textures disappear: the result looks a bit artificial.

### 3. GRAIN FILTER

One of the main characteristic of **MFCN** is its ability to preserve functions at points where roughly speaking sub- and super-neighborhoods have the same area. In contrast, it is not possible to construct simultaneously such neighborhoods near any extreme value. Either  $W^-$  or  $W^+$  are too small so that regions surrounding extrema will evolve as illustrated in Figure 3 where a  $C^1$  function becomes  $C^0$  when iterating **MFCN**.

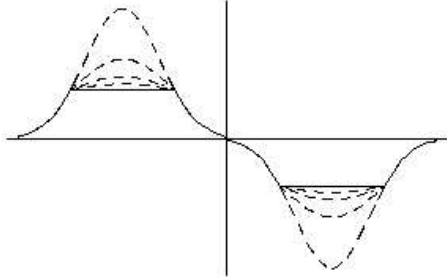


**Figure 9.** Evolution of a smooth function near the only extreme values by iterating **MFCN**.

This simple remark yields two operators, denoted by  $I_A S_A$  and  $S_A I_A$ . They were introduced by Luc Vincent in Ref. 15 within the framework of Mathematical Morphology. Basic idea is to remove connected components of level sets having small area and this can be done by combining two operators defined for every  $x$  in  $\Omega$  in the following way (algorithm can be found in Refs. 15,16):

$$I_A u(x) = \inf\{\lambda, \lambda \geq u(x), |\text{connected component of } x \text{ in } \{y \in \Omega, u(y) \leq \lambda\}| \geq A\}$$

$$S_A u(x) = \sup\{\lambda, \lambda \leq u(x), |\text{connected component of } x \text{ in } \{y \in \Omega, u(y) \geq \lambda\}| \geq A\}$$

It is easily seen that  $I_A$  acts on neighborhoods of minima of  $u$  whereas  $S_A$  acts on neighborhoods of maxima. Both filters have consequently to be combined for denoising a conventional image and they do not commute. Now, is there a possibility to process simultaneously minimal and maximal values in an image ? The following algorithm, which allows to remove grains of small area, is a possible answer:

- [1]  $u$  being an image, compute the level sets  $X_\lambda = \{y \in \Omega, u(y) \geq \lambda\}$  with respect to 4-connectivity (or equivalently the level sets  $X_\nu = \{y \in \Omega, u(y) \leq \nu\}$ ).
- [2] Let  $v$  be the topographic map of  $u$  (the set of level lines). Each level line is a union of Jordan curves (simple closed curves) enclosing a connected set with finite area (a grain). Each Jordan curve is associated with an exterior value and an interior value (it is crucial to notice that each of these curves is defined *between* pixels of image).
- [3] Compute the family of Jordan curves  $J_\alpha$  enclosing a set  $S_\alpha$  such that any other  $J_{\alpha'}$  enclosing  $S_\alpha$  is associated with a set  $S_{\alpha'}$  of area larger than or equal to  $A$ .
- [4] For every  $\alpha$ , all the points of  $S_\alpha$  are given the exterior value of  $J_\alpha$ .

Properties of this grain filter, that we shall denote by  $G_A$  in the sequel, are the following (see Ref 13 for proofs):

1.  $G_A$  is an idempotent and morphological operator depending on the only parameter  $A$ .
2.  $G_A$  is invariant with respect to any affine area-preserving mapping of the plane onto itself.
3.  $G_A$  makes the total variation decrease (the decay of total variation due to grain filter is generally smaller than the one due to  $\text{MFCN}_A$ ).
4. Like **MFCN**,  $G_A$  is associated with a large set of fixed points that can be unsMOOTH as well as smooth functions.

It is worth noticing that  $G_A$  is not increasing, in contrast to  $I_A$  and  $S_A$ . Moreover, it is equivalent to work in 4-connectivity with either sets  $X_\lambda = \{y \in \Omega, u(y) \geq \lambda\}$  or sets  $X_\nu = \{y \in \Omega, u(y) \leq \nu\}$ . But the equivalence does

not hold in 8-connectivity due to saddle-points; nevertheless,  $G_A$  still has the advantage of processing simultaneously minima and maxima, which seems more natural.

Grain filter has more and fairest properties than  $\text{MFCN}_A$ . In particular, the idempotence property implies that algorithm converges after only one iteration, which is computationally much more interesting. The results obtained with both methods are quite similar when image is slightly corrupted but they clearly differ if the quantity of noise is large ; in such a case,  $\text{MFCN}_A$  yields a “smoother” result since it converges more progressively to the solution than  $G_A$  and since every point is related to its neighbors when grain filter acts on the only extreme values.

Conventional median filter, median filter applied to some  $N_2$ -like neighborhood,  $\text{MFCN}$ ,  $I_A S_A$  or grain filter are able to remove impulse noise better than most of other denoising filters since they are closely related to occlusions removal. However, it arises from Figure 10 that conventional median filter (like median applied to  $N_2$  neighborhood) induces a smoothing effect that is very corrupting for image structure (the two crossing whiskers of the baboon have been nearly removed). In contrast, grain filter leads to a solution very close to the uncorrupted image (this is also true for  $\text{MFCN}$  and  $I_A S_A$ ). Moreover, it is easily seen that post-smoothing introduced in the last section and used in this experiment does not corrupt image globally.

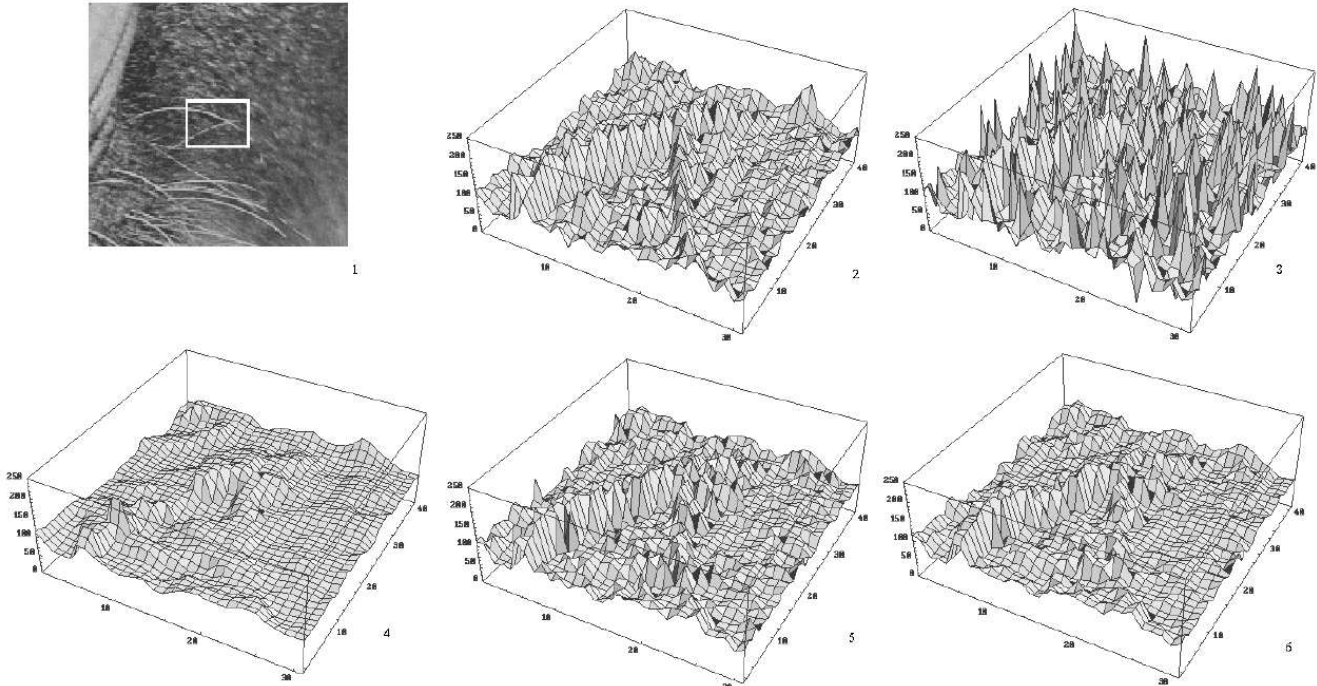


**Figure 10.** [1] Part of a baboon image [2] 3D-plot of subimage enclosed by a white rectangle in image 1  
 [3] Noisy subimage  $u$  (3D plot, impulse noise,  $f = 20\%$ ) [4]  $(\text{med}_{D(.,1.5)})^2(u)$  (3D plot)  
 [5]  $G_{10}(u)$  (3D plot) [6]  $(\text{Cmed}_{D(.,1)})^2(G_{10}u)$  (3D plot)

Both  $\text{MFCN}$  and grain filter are mainly based on the adaptation of noisy points to some underlying local coherence. This approach is particularly efficient for denoising images corrupted with impulse noise since image local coherence is more or less preserved. In contrast, any white additive noise introduces a new coherence (images corrupted with white additive Gaussian noise look quite natural) to which  $\text{MFCN}$  and grain filter shall remain fastened so that their performances are limited (see Figs. 11,12). A strong smoothing filter like Susan – but it is not morphological – is more adapted to this kind of noise because of its ability to force the construction of a coherence quite different from the one in corrupted image. The drawback is, however, that some fine details or texture may be lost. A strong smoothing effect seems actually not to be compatible with a real preservation of structures.

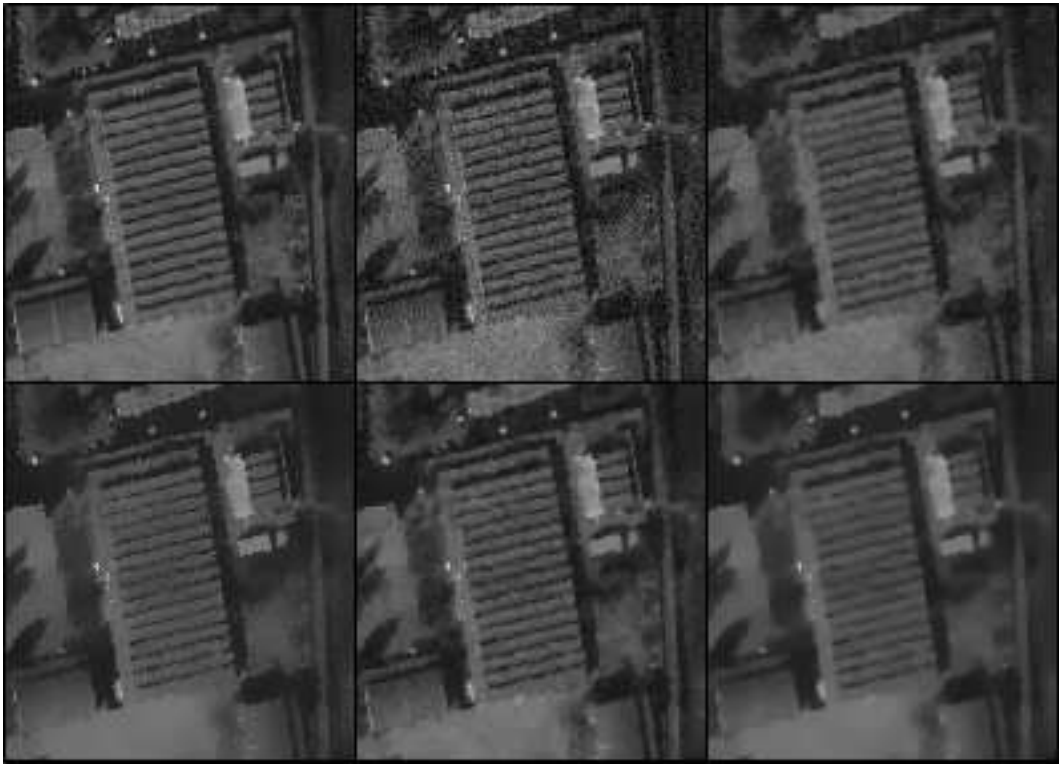


**Figure 11.** From left to right and up to bottom

1	Original image (aerial CNES photograph)	2	Noisy image $u$ (white additive Gaussian noise ; $\sigma = 10$ )
3	$G_5(\text{med}_{D(.,1)}u)$ (fixed point)	4	$(\text{Susan}_{(d=5, l=12)})^2 u$
5	Rudin-Osher ( $\epsilon = 0.5$ , $dt = 1$ ; $T_0 = 0$ ; $T_1 = 6$ )	6	Rudin-Osher ( $\epsilon = 0.5$ , $dt = 1$ ; $T_0 = 0$ ; $T_1 = 13$ )

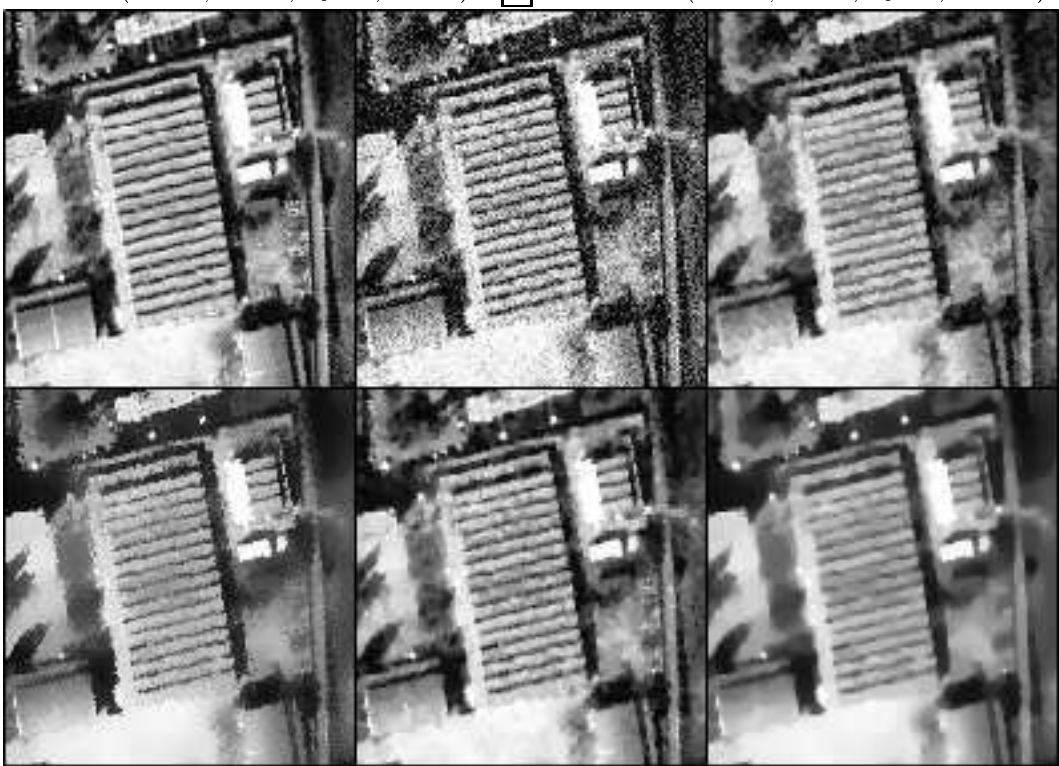


**Figure 12.** Same image as in Fig. 11 after histogram equalization

The quality of results obtained in Figs. 11,12 with Rudin–Osher global method originates, as it was already said, in the perfect designation of this method for Gaussian noise removal. The difference between images 11-5 and 11-6 shows, however, that this method is highly sensitive to the choice of parameters. Now, if we ask a denoising filter to have a small number of parameters easily adjustable, to perform well with both additive and impulse noise and to yield a fixed point, then  $\text{MFCN}$  or  $G_A$  should be preferred to Rudin–Osher method.

#### 4. CONCLUSION

In view of Leonid Yaroslavsky's work, we introduced a denoising filter,  $\text{MFCN}$ , which roughly corresponds to the computation of median value inside a neighborhood that fits perfectly at each point of image the local conformation of level lines. We also introduced a grain filter  $G_A$ , closely related to  $\text{MFCN}$ , and which derives from filters defined by Luc Vincent within the framework of Mathematical Morphology.  $\text{MFCN}$  and  $G_A$  depend on a single parameter, the area  $A$ , are morphological and remarkable in preserving image structures and shapes since both are associated with a large set of fixed points containing unsmooth as well as smooth functions. Both make the total variation decrease, the decay being more progressive and generally larger with  $\text{MFCN}$ . The choice for  $A$  being particularly easy, the two filters are perfectly designed for automation.

#### ACKNOWLEDGEMENTS

The first author thanks Leonid Yaroslavsky for useful discussions.

#### REFERENCES

1. L. Alvarez, F. Guichard, P. L. Lions, and J. M. Morel, "Axiomatisation et nouveaux opérateurs de la morphologie mathématique," *C.R. Acad. Sci Paris* **315**, Série I, pp. 265–268, 1992.
2. D. Marr, *Vision*, Freeman and Co, 1982.
3. J. F. Canny, *Finding edges and lines in images*, Master's thesis, MIT, Cambridge, USA, 1983.
4. A. P. Witkin, "Scale-space filtering," in *Proc. of IJCAI, Karlsruhe*, pp. 1019–1021, 1983.
5. J. Malik and P. Perona, "A scale space and edge detection using anisotropic diffusion," in *Proc. IEEE Comp. Soc. Workshop on Comp. Vision, Miami*, pp. 16–22, 1987.
6. L. P. Yaroslavsky, *Digital Picture Processing – An Introduction*, Springer Verlag, 1985.
7. S. M. Smith and J. M. Brady, "Susan - a new approach to low level image processing," *International Journal of Computer Vision* , 1997.
8. G. Matheron, *Random sets and integral geometry*, John Wiley and Sons, New York, 1975.
9. J. Serra, *Image analysis and mathematical morphology – Vol. 1*, Academic Press, 1982.
10. F. Guichard and J. M. Morel, "Partial differential equations and image iterative filtering," Tech. Rep. 9535, CEREMADE, Université Paris-Dauphine, France, 1995.
11. V. Caselles, T. Coll, and J. M. Morel, "A Kanizsa programme," Tech. Rep. 9539, CEREMADE, Université Paris-Dauphine, France, 1995.
12. L. P. Yaroslavsky and M. Eden, *Fundamentals of digital optics*, Birkhäuser, Boston, 1996.
13. S. Masnou, "Image restoration and pseudo-connected filters," *Preprint* .
14. L. Rudin and S. Osher, "Total variation based image restoration with free local constraints," in *Proc. of the IEEE ICIP-94, Austin, Texas*, vol. 1, pp. 31–35, 1994.
15. L. Vincent, "Morphological area openings and closings for gray-scale images," in *Proc. of the Workshop "Shape in Picture", 1992, Driebergen, The Netherlands*, pp. 197–208, Springer-Berlin, 1994.
16. H. Heijmans, "Introduction to connected operators," in *Non linear filters in Image Processing*, E. Dougherty and J. Astola, eds., SPIE Optical Engineering Press, 1997.